Evolution of crystallographic preferred orientations in flowing polycrystalline ice: A continuum modelling approach validated against laboratory experiments

Daniel Richards, Sam Pegler, Sandra Piazolo, Oliver Harlen
Flud Dynamics CDT, University of Leeds

1. Introduction

- Mass loss from ice sheets in Greenland and Antarctica is expected to be the dominant contributor to sea level rise in this century.
- A key facet of understanding ice flow is understanding how the microstructure evolves in flowing ice.
- A key feature of the microstructure which controls the rheology is the collective distribution of crystallographic c-axes in the ice, called the *crystallographic preferred orientation* (CPO).
- Here we provide the first fully-constrained model, validated against experiments, to predict the evolution of the CPO including all processes shown below:

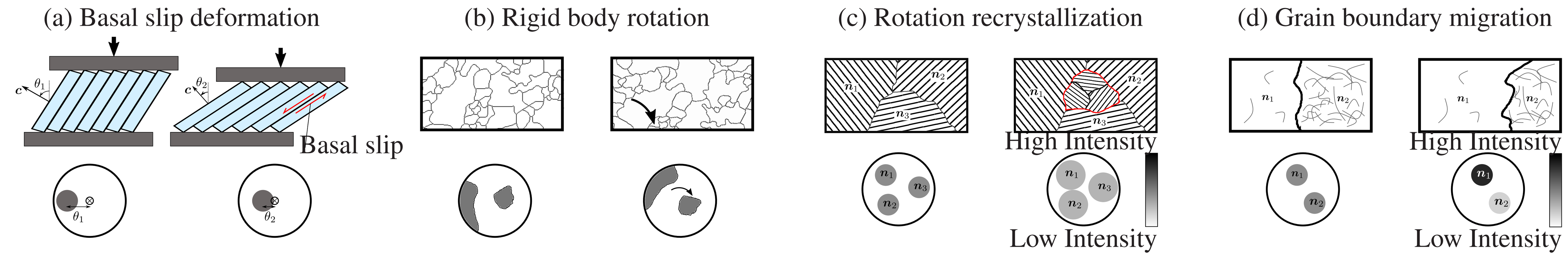

Figure 1: Schematic of microstructural processes which affect the CPO, and also the corresponding affect on a distribution function of c-axes, visualised with a pole figure.

2. CAFFE Model and Spectral Method

- To model the CPO evolution we use half of the CAFFE model (Placidi et al., 2010), which includes all processes shown in fig. 1.
- We solve the CAFFE model using a novel (in the glaciological context) spectral method from Montgomery-Smith et al. (2010) which can solve this equation to high accuracy with low computational cost.
- We non-dimensionalise the CAFFE model for ice deformed in a laboratory, based on the strain-rate and density of the deformed ice:

$$\frac{\partial \tilde{\rho}^*}{\partial \tilde{t}} = -\nabla^* \cdot [\tilde{\rho}^* \tilde{\boldsymbol{v}}^*] + \overbrace{\tilde{\lambda} \nabla^{*2}(\tilde{\rho}^*)}^{\text{fig. 1c}} + \overbrace{\tilde{\rho}^* \tilde{\beta}(\mathcal{D}^* - \langle \mathcal{D}^* \rangle)}^{\text{fig. 1d}}$$

where

$$\tilde{v}_i^* = \underbrace{\tilde{W}_{ij} n_j}_{\text{fig. 1b}} - \underbrace{\iota[\tilde{D}_{ij} n_j - n_i n_j n_k \tilde{D}_{jk}]}_{\text{fig. 1a}}.$$

- $\iota(T)$ controls the ratio of basal slip deformation to rigid-body rotation
- $\tilde{\lambda}(T)$ controls the ratio of rotation recrystallization rate to strain rate
- $\tilde{\beta}(T)$ controls the ratio of grain boundary migration rate to strain rate

We provide a first constraint of these three non-dimensional parameters $\iota, \tilde{\lambda}, \tilde{\beta}$ as functions of temperature.

3. Inversion from Simple Shear

- The model was inverted to find the set of parameters $\iota, \tilde{\lambda}, \tilde{\beta}$ which best fit CPOs from experiments in simple shear (Qi et al., 2019; Journaux et al., 2019).
  - This was done by minimising the error between experiments and the model for the fourth-order orientation tensor.
  - Figure 2 shows the parameters found from this inversion at $-30, -7, -5°$ C. A linear fit is calculated to give $\iota, \tilde{\lambda}, \tilde{\beta}$ as functions of temperature..

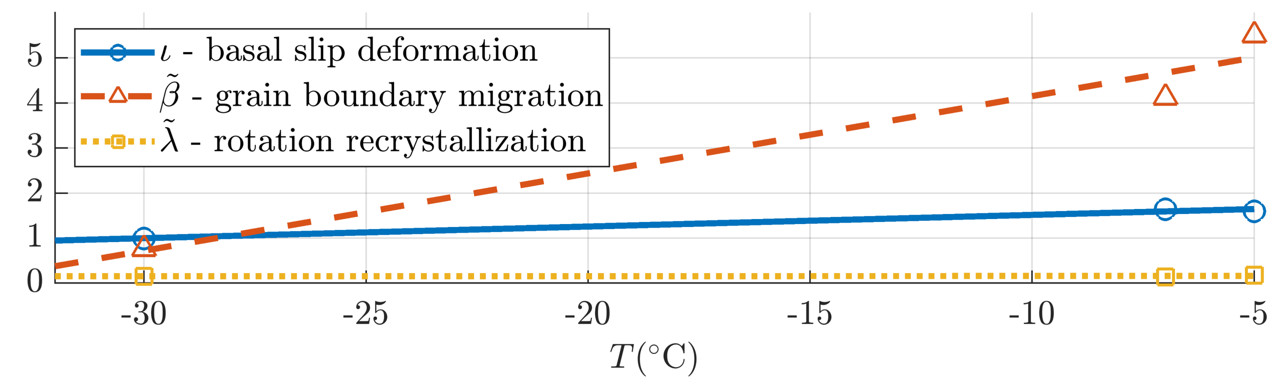

Figure 2: Plot of parameters as functions of temperature, found by fitting the outputs of the model to experimental data in simple shear from Qi et al. (2019) and Journaux et al. (2019)

.

- Figure 3 shows a comparison between the model prediction and experiments performed by Qi et al. (2019) at $-5°$ C.
  - The model with these parameters accurately tracks the evolution of the second order orientation tensor $\mathbf{A}^{(2)}$ as strain increases.
  - The experimental CPO which is plotted as a diamond in fig. 3a is shown as a pole figure in fig. 3b.
  - We accurately reproduce the secondary cluster - this is made possible by including grain boundary migration correctly.

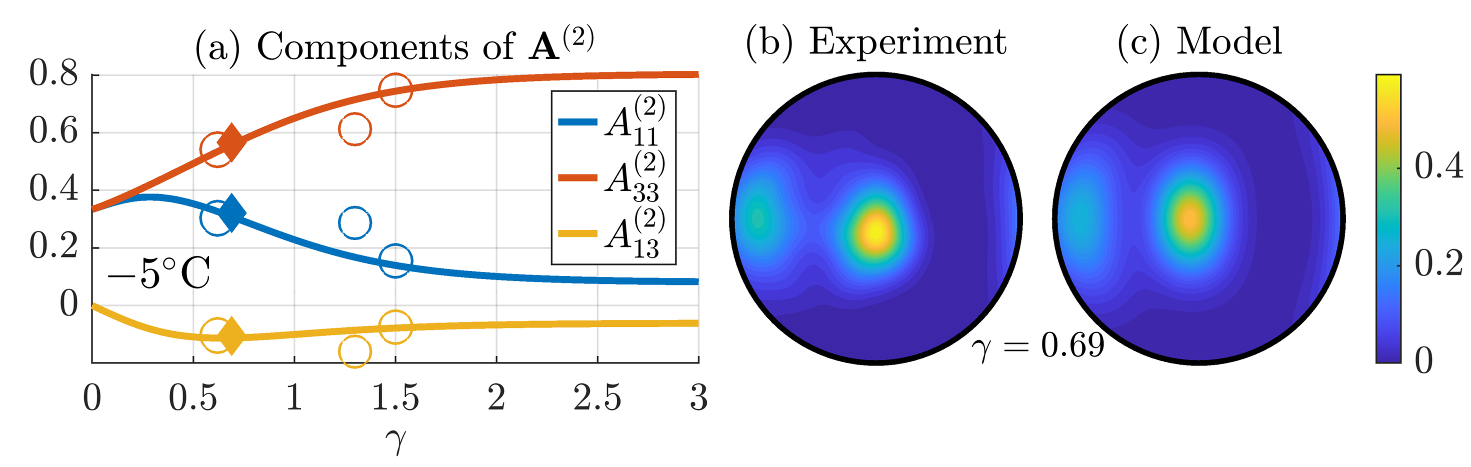

Figure 3: Comparison of model and experiments at $-5°$ C in simple shear. A plot of components of the second-order orientation tensor for the model alongside experimental data points is shown. The experiment represented by diamond point corresponds to the leftmost pole figure. The CPO from the model is shown at the same strain.

4. Extrapolation to Compression

- We apply the model and parameters-as-functions-of-temperature to a different flow state: unconfined vertical compression
- Here no fitting is performed - the results come using parameters found in simple shear.
- Figure 4 shows excellent agreement between experimental data points and the model and parameters, across a range of temperatures.
- We are also able to accurately reproduce the cone-angle seen in experimental CPOs.

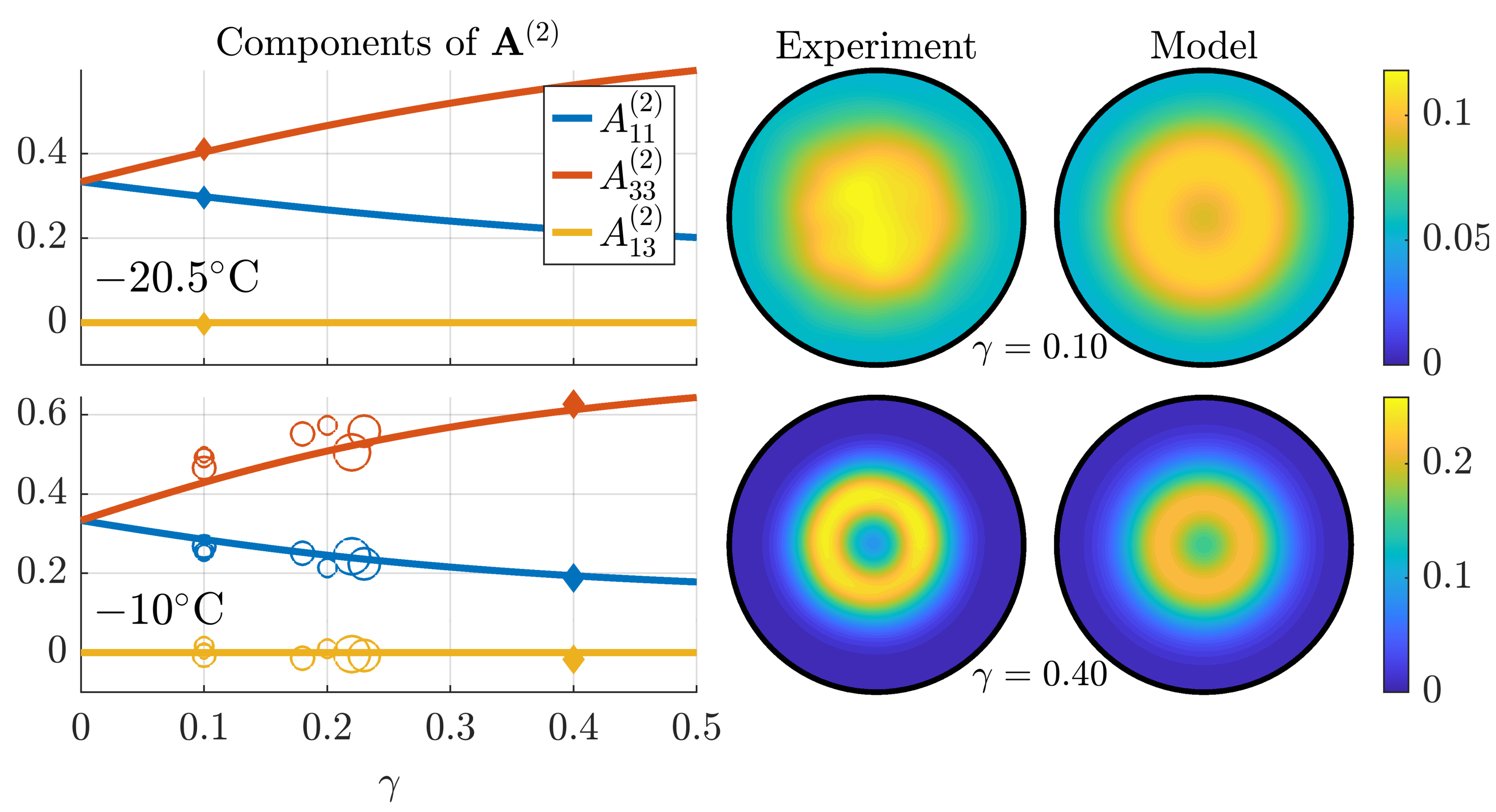

Figure 4: Comparison of model and experiments in unconfined vertical compression. A plot of components of the second-order orientation tensor for the model alongside experimental data points is shown. The experiment represented by diamond point corresponds to the leftmost pole figure. The CPO from the model is shown at the same strain.

5. Key Results & Outlook

- By inverting the model against laboratory experiments in simple shear we we find the first values for the quantitative importance of recrystallization processes as functions of temperature.
- These inverted parameters from simple shear are then applied to compression, and agree excellently with experimental results.
- The combination of the model, the spectral method and parameters as a function of temperature are able to give accurate predictions of ice crystal fabric evolution in any condition.
- This approach can be applied to both large scale ice sheet flows, and to provide greater understanding of ice microstructure and ice-core interpretation.

References

Placidi et al. 2010, Continuum Mechanics and Thermodynamics, 22, 221. Montgomery-Smith et al. 2010, Composites Part A: Applied Science and Manufacturing, 41, 827. Qi et al. 2019, The Cryosphere, 13, 351. Journaux et al. 2019, Recrystallization processes, microstructure and texture evolution in polycrystalline ice during high temperature simple shear.